

Conceptual Design and Analysis of a Multi-Functional UAV

Abhishek Jadhav ¹, Devraj Bhosale ², Pandi Siddharth ³, Sunil V. Dingare ⁴

¹ Final year student, Department of Aerospace Engineering, MIT SOE, MIT ADT University Pune, INDIA

² Final year student, Department of Aerospace Engineering, MIT SOE, MIT ADT University Pune, INDIA

³ Assistant Professor, Department of Aerospace Engineering, MIT SOE, MIT ADT University Pune, INDIA

⁴ Professor and Head, Department of Aerospace Engineering, MIT SOE, MIT ADT University Pune, INDIA

ABSTRACT

Since past decade, there has been a drastic increase in the UAV technology to cope up the ever increasing demand of new and improved solutions for already existing problems. Making use of an aerial vehicle for jobs such as traffic monitoring, [1] payload delivery, [2] military surveillance, agricultural and industrial survey is far more time and cost efficient than having to do the same manually. [3] Moreover, automating these tasks with unmanned aerial vehicles takes the efficiency to another level wherein, a UAV can be programmed to map out a particular area to gather data without any human intervention. This automation helps to complete long and tedious task with utmost precision and real-life results.

[4] This has now become a trend to use a UAV for such applications which has led the UAV market to rise more than \$45 Billion value in past few years. It has made the DGCA to implement new laws and regulations for aviation of these UAVs.

While considering the above applications and possibilities, [5] the UAV enthusiast have been managing to come up with more unique ways to use this technology for betterment of humanity. This thesis shows yet another unique advancement in the UAV technology that could open doors for using this system for multi-tasking.

Keyword: - UAVs, multi-functional, applications, autonomous, cheap & accurate..

1. INTRODUCTION

UAV technology is an emerging field for the innovators to make scientific breakthrough. The applications such as, remote sensing, real-time monitoring, [8] civil infrastructure inspection, providing wireless coverage, search and rescue, [9] precision agriculture, are now possible to be carried out by not only large-scale businesses, but also by small-scale emerging firms at cheaper costs. This has indirectly helped the humankind to progress in wider fields due to availability of massive and accurate data gathering solutions at cheap.

While considering the above mentioned examples and taking a look at the wide verity of possibilities, it can be assumed that there is a UAV for almost every aspect of field. A UAV powered by the solar energy that can travel throughout the globe to function like a satellite for transmitting signals. UAVs to explore any inaccessible terrains which otherwise for humans would be risky to approach. This technology has made possible for researchers to carry out risky operations with ease.

Excluding the above applications which are suited for long-distance travelling, there are UAVs that are capable of carrying out short term precise manoeuvres as well. UAVs that can map out certain areas, and locate appropriate land for farming. By equipping these UAVs with ultrasonic sensors and LiDARs, they get the ability to determine their altitude with respect to variation in topology. This system is used to monitor crops over a period of time and generate growth reports for production analysis, do local fixed target surveillance in stealth, transport supplies at precise locations.

All of these applications being at the state of the art level, has a specific limitation. These UAVs are constrained to their specific tasks and their mission profiles. This project focusses on the multi-functional aspect of UAVs. Making

use of existing facts of flight dynamics, a new system is designed to manipulate the UAV structure in real-time flight to achieve multi-functionality for a single system.

1.1 MOTIVATION

The main motivation of this project is to use already existing technology to achieve something new. Making a UAV multi-functional would minimize the time and cost of production, operation and maintenance. Having a system carry out short-range precise and long-range tougher operations would help shorten the time and cost of flights, thus increasing the level of achievements.

1.2 LITERATURE SURVEY

The purpose of literature survey for this project was to understand the applications, the need, the trends, and the future of UAV industry.

A. Outcomes of the survey:

- Types of UAVs and their uses.
- Regulations and guidelines for flying UAVs.
- Flow visualisation over swept wing.
- CFD using open-source software.
- References for initial constraints.

Having done the literature survey, we got a better understanding of the functioning UAVs and what aspects are to be considered while analysing a UAV.

B. Research goal:

In general, an aircraft will be faster, the lesser drag it generates. And it can achieve longer distances as larger surface area it has. Keeping this basic concept in mind, the goal of this project is to design a system, that can be manipulated in flight, to change its wing surface area to suite the mission requirements. This gives the control to use the same system for multiple functions in same mission profile.

C. General plan:

To achieve the design that is intended, the plan is to first find an existing UAV that can be then compared with, in terms of its weight, payload capacity, range and endurance for the requirement of historical data that is needed to design an aircraft from scratch. The UAV that suites the best for the purpose of this project is, the PENGUIN-C UAS by UAV Factory. This aircraft is referred throughout this project for calculations of the initial sizing, constraint analysis, landing system, etc.



Fig. 1. PENGUIN-C UAS (Source – UAV Factory)

Once, the initial parameters are decided, a CAD model can be designed based on these parameters. This CAD model will then be used to carry out initial CFD analysis to determine the performance of UAV in its initial stage. Based on these results, the model will then be optimised for best performance while considering every parameter. And the CAD model will be refined to carry out the final CFD analysis using two different techniques and tools to verify the results.

2. DESIGN

This is a design of a UAV which allows us to manipulate its mission profile dynamically while in the air. It has two flying modes that can be set according to mission requirements.

- Mode 1: Long-range mode
- Mode 2: High-speed mode

These two modes are achieved by changing the wing sweep.

A. Working:

Mission profile for this UAV can be varied according to the mission requirement. Mode 1 is used for long-range mission profiles and Mode 2 is used for short but high-speed mission profiles.

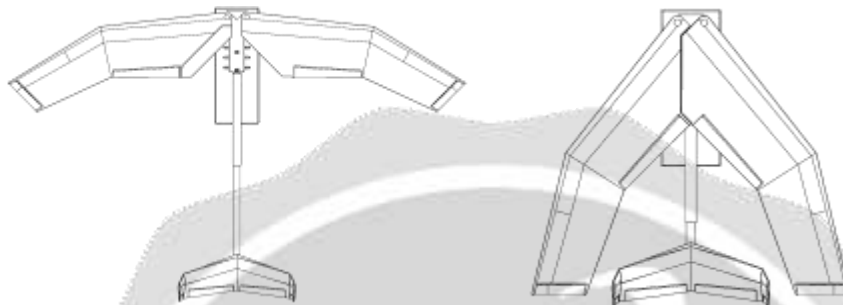


Fig. 2.Mode 1 & Mode 2

A.1 Mode 1:

This mode has a higher aspect ratio and thus helps to increase lift generation. The main purpose of this mode is to increase the wing surface area to generate more lift. The UAV functions more like a glider while in this mode. It helps to get higher values of glide ratio.

Say, if 20:1 is the glide ratio of an aircraft, it means that it can glide up to 20 km while at a distance of 1 km above the ground before eventually touching down. Using this principle, it can drastically increase the range, keeping the power requirements low.

A.2 Mode 2:

This mode has a higher sweep angle and thus helps to decrease drag generation. The sweep angle helps the UAV to travel at higher speeds without worrying too much about turbulence when speed abruptly changes. [10] Stability is another crucial role played by the swept-back wings. In an aircraft wings, there is a low pressure area on top of the wings than on the bottom. Meaning, the airspeed on top of the wing is slower and thus helps to generate the lift. But as the velocity of aircraft starts to increase, the airflow on top of the wing increases abruptly which leads to vibration of the body. In case of swept-back wings, it creates an imaginary increase in the wingspan. Thus, the air is under an illusion that the velocity of the aircraft is less than its actual velocity. This results in fewer vibrations, thereby increasing the lateral stability.

B. Parameters:

B.1 Initial sizing:

The initial sizing/weight of the UAV is 23.29 kg

1.	Endurance	20 hrs
2.	Range	100 km / 60 miles
3.	Payload	approx. 10 kg
4.	Ceiling	4500m/15 000 ft

Table I. Initial Sizing

B.2 Constraint analysis:

$$\frac{P}{W_{SL}} \geq 0.1969 \ \& \ \frac{W}{S} \leq 17.736 \text{ kg/m}^2$$

B.3 Fuselage sizing:

1.	Fuselage length	0.5697 m
2.	Fuselage diameter	0.1864 m
3.	Fuselage Fineness Ratio	3.0562
4.	Coefficient of drag	0.3272

Table II. Fuselage Sizing

B.4 Wing dimensions:

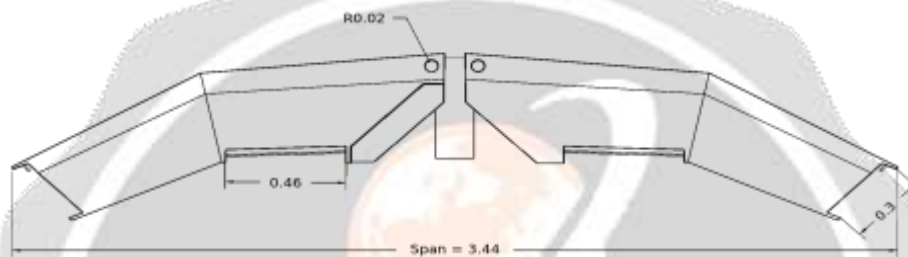


Fig. 3. Wing dimensions

1.	λ_{wing}	0.64
2.	Wingspan	3.44 m
3.	AR	8.37
4.	t/c	15 %
5.	Λ	20°
6.	Setting angle	3°
7.	Area	1.4 m ²

Table III. Wing Dimensions

The wing has two different sweep angles:

- The inner sweep is kept minimum as it is the major lift generating part.
- The outer wing has larger sweep as it is designed for maintaining stability of the UAV.

B.5 Tail dimensions:

The tail is designed to be H-tail configuration for,

- CG location is in the front. So, to maintain its stability in directional axis, two vertical tails are used to handle the unbalanced forces, as it increases the surface area for vertical tail.

- The forces are distributed between two vertical tail, instead on a single vertical tail.

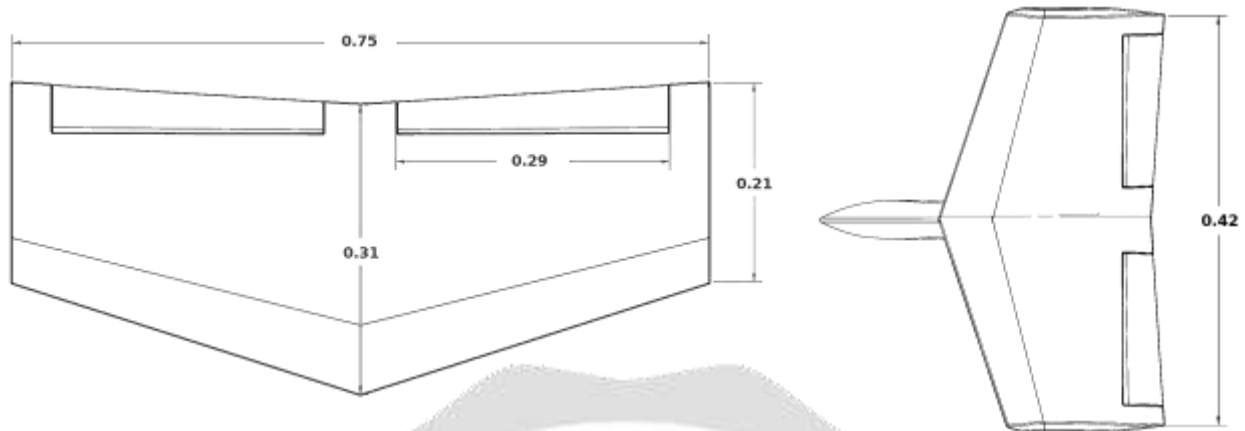


Fig. 4. Tail dimensions

Horizontal tail			Vertical tail		
S. No.	Parameters	Dimensions	S. N0.	Parameters	Dimensions
1.	λ_{wing}	0.67	1.	λ_{wing}	0.5
2.	Wingspan	1.0 m	2.	Wingspan	0.42 m
3.	AR	2.34	3.	AR	1.76
4.	t/c	12 %	4.	t/c	12 %
5.	Λ	10°	5.	Λ	35°
6.	Area	0.24 m2	6.	Area	0.10 m2

Table IV. Tail Parameters

C. Engine selection:

[12] There are two options that can work very well with this UAV- Electric (battery powered) or Fuel powered engine. As this UAV is lightweight (24 kg), battery powered engine can prove to be more advantageous for this design.

- One of the modes for this UAV is long-range. To achieve this, we need as much fuel capacity as possible. [13] Using a battery powered engine, we have the advantage to generate more charge in flight by, either covering the wing tops with thin solar films or by attaching a small sized propeller which can drive a shaft to generate charge. (These options would be used for secondary power supply).
- No discharge of burnt gases, meaning no air pollution.
- Easy to do regular maintenance, as this system is not as complicated as fueled engines.

D. Landing system:

The UAV designed in this project does not have wheels for take-off and landing. It is launched using spring-loaded launch catapult and landed using parachute recovery. Implementing these features helps to reduce the weight for landing gear which can be utilized by the payload.

The landing system works in 4 steps:

1. Deploying the drogue chute.
2. Deploying the main chute container.
3. Opening the main chute and Descent of the UAV.

E. Control surfaces:

As the UAV is designed to fly in two modes, the configuration of the aircraft changes in both modes. Thus the usage of control surfaces is specific for the specific mode.

- In mode 1, the inner control surfaces of the wing acts as the ailerons and are responsible for rolling action.
- In this mode, the outer control surfaces of the wing acts as the ailerons and are responsible for rolling action.
- The tail has 6 control surfaces. As the front part of the UAV is heavy, meaning cg of aircraft is towards the front, a huge amount of force has to be generated by tail to keep the aircraft stable. Thus, there are two vertical tails instead of just one. This helps in directional stability.

3. METHODOLOGY

The main idea is to use two open-source software to analyze results using two different methods. The two software are – OpenFOAM and OpenVSP. The plan is to carry out CFD analysis to achieve the most optimized results. This depends on assigning the appropriate values to geometric parameters.

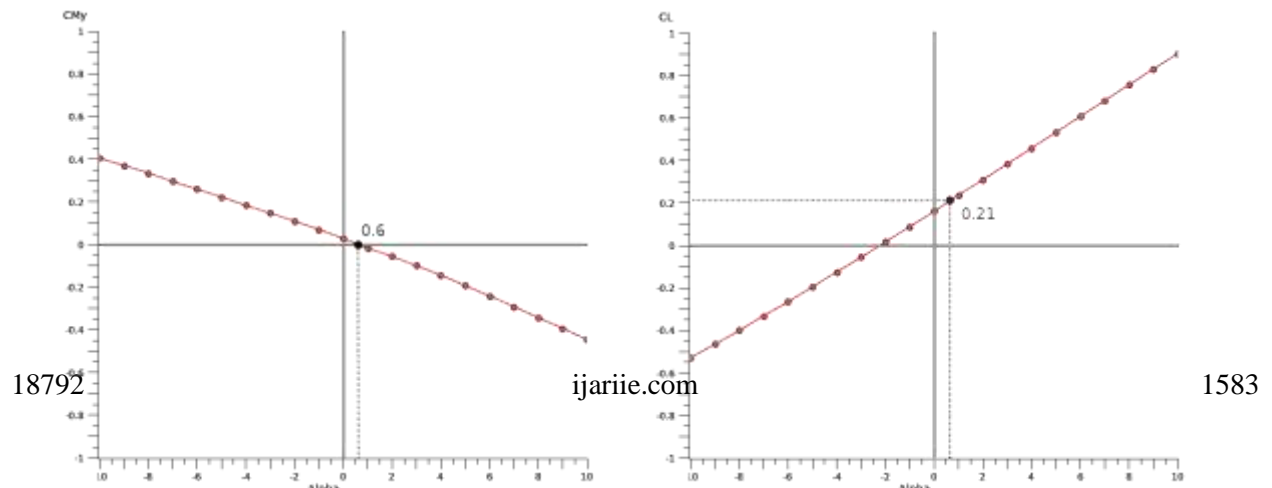
- **OpenFOAM:** OpenFOAM is an open-source software which calculates the aerodynamic parameters using FEM, FDM, or FVM methods. It does the discretization of a given CAD model and divides it into finite number of elements and applies the PDEs to every element to calculate the aerodynamic parameters. Thus, this method requires long calculation time and high computational power. But the results achieved using this method are more accurate compared to OpenVSP.
- **OpenVSP:** OpenVSP is an open-source software which calculates the aerodynamic parameters using VLM method. It takes the geometric parameters such as wing area, AR, sweep angle, etc. and creates a CAD model using these parameters to calculate the aerodynamic parameters. Thus, this method requires comparatively lesser calculation time and lower computational power. But the results achieved using this method are less accurate as compared to OpenFOAM.

S. No.	OpenFOAM	OpenVSP
1.	FEM, FDM, FVM	VLM, Panel Method
2.	Discretization	Geometric parameters
3.	Very long calculation time	Short calculation time
4.	High computational requirements	Medium computational requirements
5.	More accurate	Comparatively less accurate

Table V. SOLVERS COMPARISON

Both the above mentioned software have their own advantages. In this project, OpenVSP is used to do initial analysis as it uses Vortice Lattice Method for calculating force coefficients, which is much faster and simpler to set up than Finite Volume Method. OpenVSP is designed by NASA specifically for analyzing conceptual designs, as the design parameters has to be changed constantly and needs to have iterative process for achieving optimized results.

The plan is to optimize the design using OpenVSP to get relative parameters and use these parameters to



refine the CAD model for OpenFOAM simulation as final result. Results from both solvers will be compared to check errors and solver compatibility.

Fig. 5. Cm-Alpha graph, Cl-Alpha graph (Wing setting angle = 0°)

The above figure (fig. 5) shows the values of Cl at various angles when wing setting angle is set to 0°. It is seen that at $\alpha = 0.6^\circ$, neutral point is achieved. And the corresponding Cl value is 0.21.

Similarly, the fig. 6 shows the values of Cl at various angles when wing setting angle is set to 3°. It is seen that at $\alpha = 2^\circ$ neutral point is achieved. And the corresponding Cl value is 0.5.

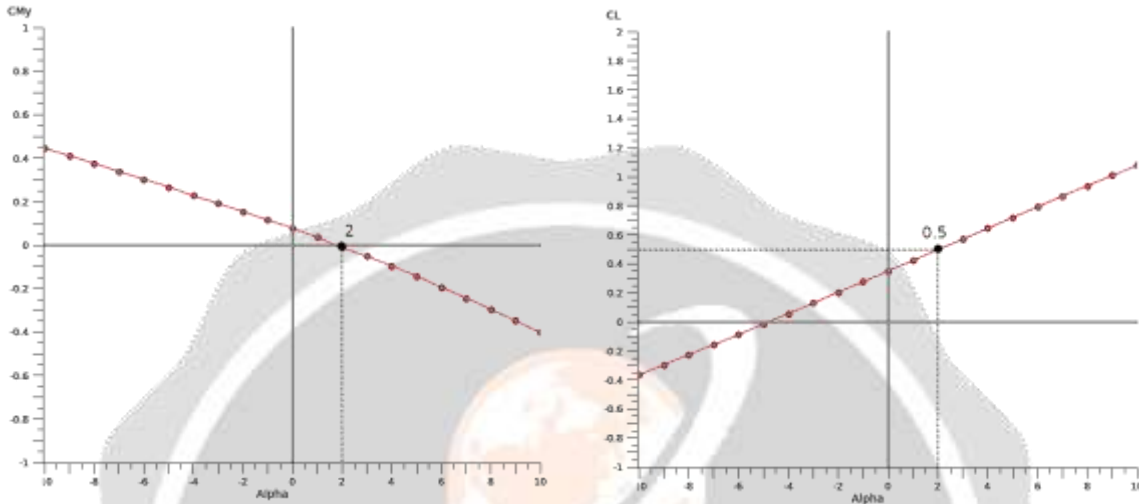


Fig. 6. Cm-Alpha graph, Cl-Alpha graph (Wing setting angle = 3°)

When we compare the Cl values for both cases, it is seen that by changing just the wing setting angle, a big difference is achieved. This is just to show that just changing a single geometric parameter can lead to many changes in the results.

Thus, there are many geometric parameters to be considered to optimize the design. Such as,

- Wing: angle, AR, area.
- Tail: angle, AR, area, moment arm, elevator deflection.
- CG location (accordingly positioning the payload).
- Airfoil.

But while manipulating these values, there are certain parameters that remain the same in both the modes, while some change by changing the mode from high-speed to long-range. This adds a new level of complexity to set specific values that should work better in both the modes. These parameters include,

- Wing area, tail area, tail AR, setting angle for wing and tail remain same.
- Wing AR, CG location, tail moment arm, neutral point change.

Thus our methodology is to set the perfect values to these geometric parameters which in turn would result in the most optimized design for this UAV.

4. ANALYSIS & VALIDATION

In order to prove the accuracy of the solvers of both the software in this project, their results has to be validated with some form of proven results. For the purpose of this project, we have chosen a [16] research paper published on Research Gate dated April 2013.

Authors – Shinde, Subhash & Paul, Akshoy & Jain, Anuj

A. About the paper:

The objective of this paper was to compare the results of a delta-rectangular wing, designed and analyzed in Ansys Fluent with the real-world results of the same wing tested in NASA's wind tunnel in 1981. The paper shows the output of the software and the wind tunnel results. And the results obtained are found to be in good agreement with wind tunnel test results.

B. Wing design:

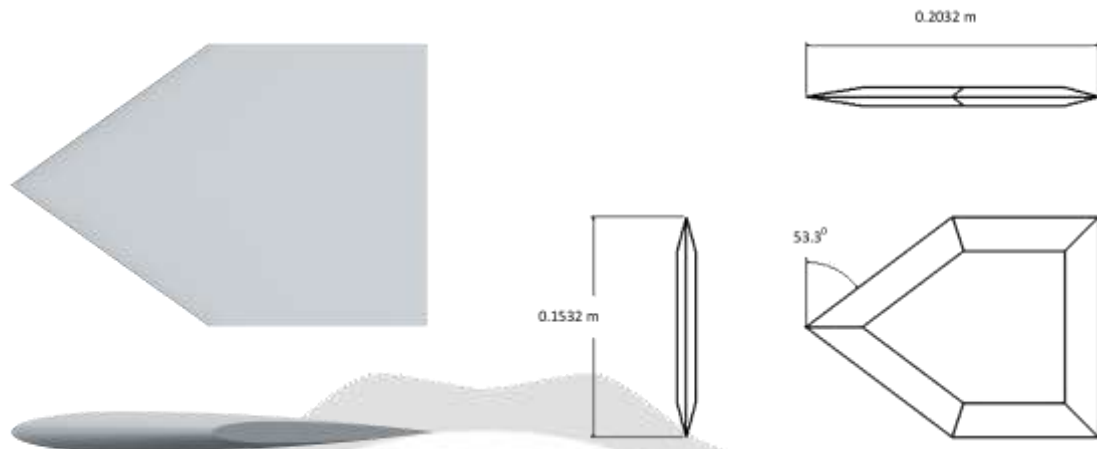


Fig. 7. Rectangular delta wing

Fig. 7 shows the wing dimensions used in the research paper. Using these parameters, a CAD model is designed on which the solvers will be tested.

C. Process:

C.1 OpenVSP:

Firstly, the geometry is created and interpolated to create divisions for the solver to identify the geometric parameters. Fig. 8 shows the geometry and the interpolations. There 6 divisions made in the span length with zero bias factor, meaning, the interpolations are spread across uniformly throughout the span but biased along the chord to capture the leading and trailing edges.

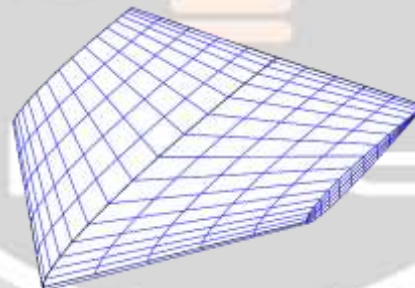


Fig. 8. Geometry

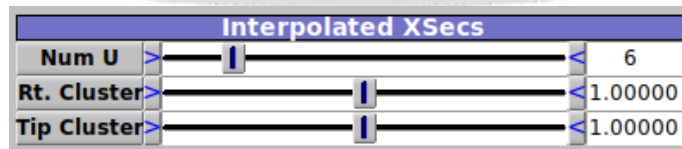


Fig. 9. Interpolation values

Then, the case is set up to use the Vortex Lattice Method (Fig. 10). VLM is generally used for the early stage aircraft design process for fast calculations without considering any turbulence effects, enabling to iterate and find optimal parameters. VLM considers the lifting surfaces of an aircraft as an infinitely thin sheet having discrete vortices to calculate force coefficients without considering the viscosity.

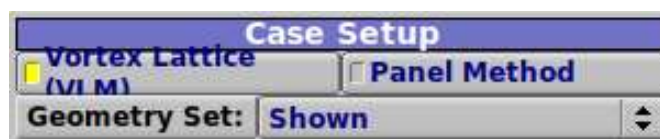


Fig. 10. Case setup

After setting up the case, the CG has to be set to calculate coefficient of moment (Fig. 11). This can be calculated using the geometry distribution. Finally, the flow conditions has to be specified. This is the information about the variance of angle of attack from its initial to final value. Number of steps to interpolate between these values is also specified. Calculations will be done on every step between the initial and final values. The flow velocity is also set (Fig. 12). In this case, according to research paper, the velocity is set to 1.6 Mach.

Moment Reference Position	
Mass Set:	Calc CG
Num Slices	10
Xref	0.108
Yref	0.000
Zref	0.000

Fig. 11. Adjusting CG

Flow Condition					
Alpha Start	0.000	End	10.000	Npts	10
Beta Start	0.000	End	0.000	Npts	1
Mach Start	1.600	End	0.000	Npts	1

Fig. 12. Flow conditions

C.2 OpenFOAM:

OpenFOAM is a terminal based application. It does not have any user-interface. Following are the commands, their input values and their specifications used to solve this case:

```

convertToMeters 1;

vertices
(
  (-2 -3 -1.5)
  ( 6 -3 -1.5)
  ( 6  3 -1.5)
  (-2  3 -1.5)
  (-2 -3  1.5)
  ( 6 -3  1.5)
  ( 6  3  1.5)
  (-2  3  1.5)
);

blocks
(
  hex (0 1 2 3 4 5 6 7) (45 45 35) simpleGrading (1 1 1)
);

```

Fig. 13. Grading

C.2.a Block Mesh:

This command is used to,

- Creating domain around the model (fig. 13)
- Initial grading of the block

- Assigning boundary patches (fig. 14)

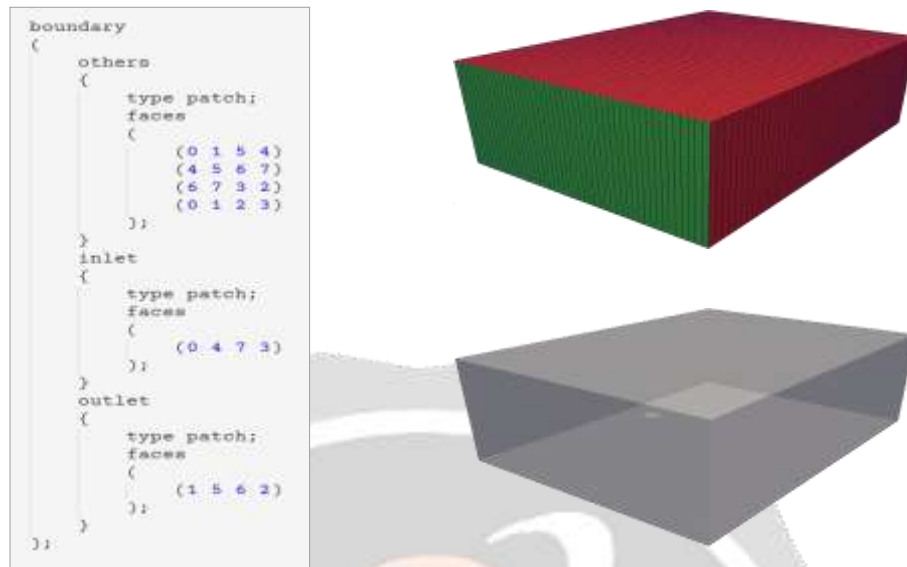


Fig. 14. Patches and domain

C.2.b. Surface Features:

This command is used to,

- Extract the surfaces and edges of the CAD model
- Prepare the geometry for meshing
- Generates. eMesh file for the next command to read the geometry

```

surfaces ("validation.obj");

// Identify a feature when angle between faces < includedAngle
includedAngle 150;

subsetFeatures
(
  // Keep nonManifold edges (edges with >2 connected faces)
  nonManifoldEdges no;

  // Keep open edges (edges with 1 connected face).
  openEdges yes;
)

```

Fig. 15. Surface features

C.2.c Snappy Hex Mesh:

This command is used to,

- Create volume mesh
- Subtract geometry
- Snap cells to match geometry
- Initialize boundary conditions

```

// Which of the steps to run
castellatedMesh true;
snap true;
addLayers false;

```

```
locationInMesh (-1 0 0);
```

Fig. 16. Setting suitable algorithm

Fig. 17. Refinement box

```

geometry
{
  validation
  {
    type triSurfaceMesh;
    file "validation.obj";
  }

  refinementBox
  {
    type searchableBox;
    min (-0.8 -1.0 -0.8);
    max ( 2.0  1.0  0.8);
  };
};

castellatedMeshControls
{
  features
  {
    {
      file "validation.eMesh";
      level 3;
    };
  };
};

```

Fig. 18. Refinement level

```

refinementSurfaces
{
  validation
  {
    // Surface-wise min and max refinement level
    level (5 6);

    patchInfo
    {
      type wall;
      inGroups (UAVGroup);
    }
  }
};

refinementRegions
{
  refinementBox
  {
    mode inside;
    levels ((1E15 4));
  };
};

```

The following fig. 19 shows the difference before and after applying the snapping algorithm. Before the algorithm is executed, the volume mesh is created, but the centers of the cells are arranged on the surfaces of the geometry. Due to this the mesh is not clean, as the edges of the cells are not yet snapped properly. But after the snapping, the cell edges detect the geometry surfaces and get arranged accordingly to capture the surface.

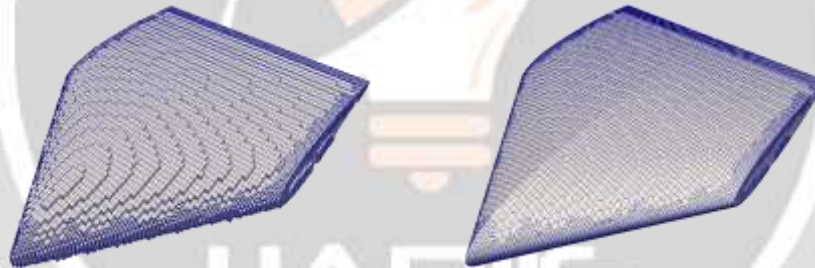


Fig. 19. Before and after snapping

C.2.d. Initialization:

This is done to,

- Set turbulence & transport model
- Set inlet flow velocity (m/s)
- Set convergence criteria
- Set control parameters

The turbulence model used in this validation is k-omega-SST and the transport properties are set to Newtonian (fig. 20). The inlet velocity is 555 m/s. The solver uses SIMPLE algorithm. The simulation starts from zero with a time-step of 1 (fig. 21). The convergence criteria for all the parameters is set to 10⁻⁶.

```

simulationType RAS;

RAS
{
    model            kOmegaSST;

    turbulence       on;
}

////////////////////////////////////

transportModel  Newtonian;

nu              [0 2 -1 0 0 0 0] 1.5e-05;

////////////////////////////////////

flowVelocity    (555 0 0);

```

Fig. 20. Flow conditions

```

application    simpleFoam;

startFrom      latestTime;

startTime      0;

stopAt         endTime;

endTime        10000;

deltaT         1;

writeControl   timeStep;

writeInterval  50;

purgeWrite     0;

writeFormat    binary;

writePrecision 6;

writeCompression off;

timeFormat     general;

timePrecision  6;

runTimeModifiable true;

solvers
{
    P
    {
        solver      GAMG;
        smoother    GaussSeidel;
        tolerance    1e-6;
        relTol      0.01;
    }

    U
    {
        solver      smoothSolver;
        smoother    GaussSeidel;
        tolerance    1e-6;
        relTol      0.1;
        nSweeps     1;
    }

    k
    {
        solver      smoothSolver;
        smoother    GaussSeidel;
        tolerance    1e-6;
        relTol      0.1;
        nSweeps     1;
    }

    omega
    {
        solver      smoothSolver;
        smoother    GaussSeidel;
        tolerance    1e-6;
        relTol      0.1;
        nSweeps     1;
    }
}

```

Fig. 21. Solver control & Convergence criteria

D. Results:

The residuals for all the parameters are converged at 10^{-6} (fig. 22). Fig. 23 shows the pressure distribution throughout the wing. A low pressure area is observed on the top. The Cl value has been converged at 0.16.

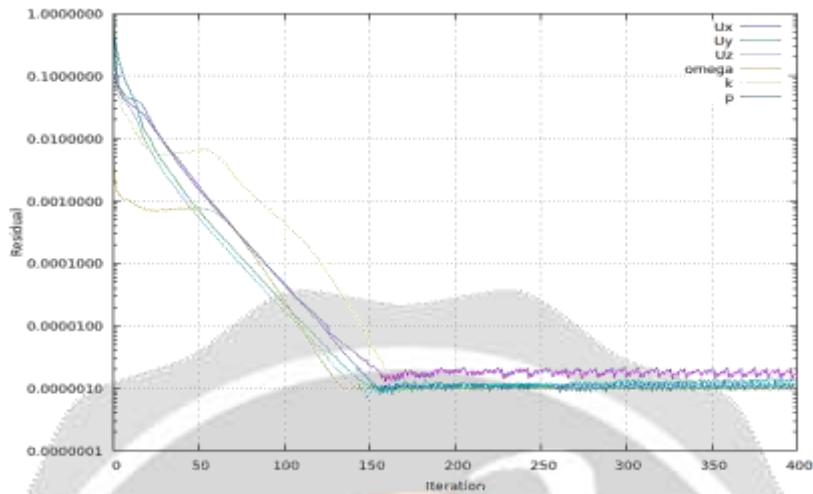


Fig. 22. Residual Plot

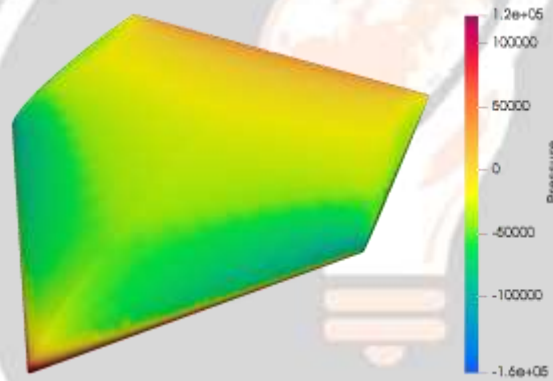


Fig. 23. Pressure distribution

E. Comparison of results:

In this section, the results from the research paper, results obtained from OpenVSP and the results obtained from OpenFOAM are compared to check the validity of solvers.

Research Paper		OpenVSP		OpenFOAM	
Alpha	Cl	Alpha	Cl	Alpha	Cl
5°	0.18	5°	0.19	5°	0.16
10°	0.35	10°	0.38	10°	0.33

Table. VI. Solvers Result Comparison

Fig. 24, 25, 26 shows the C_L - α graphs for all three criteria.

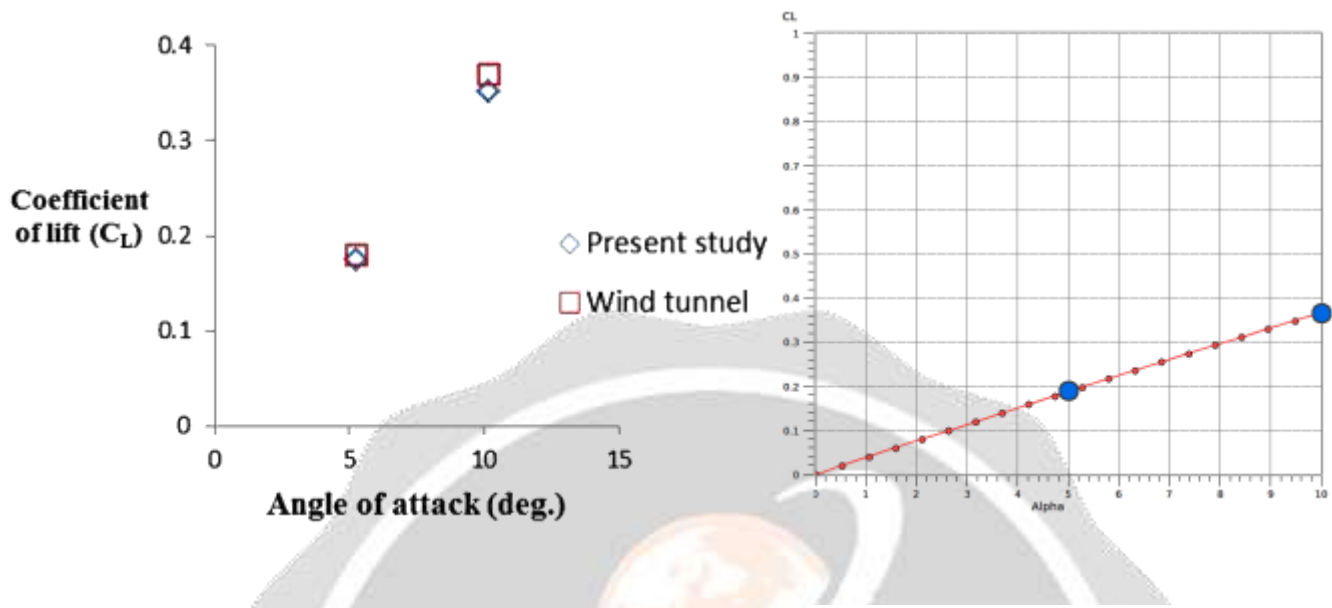


Fig. 24. Research paper graph

Fig. 25. OpenVSP

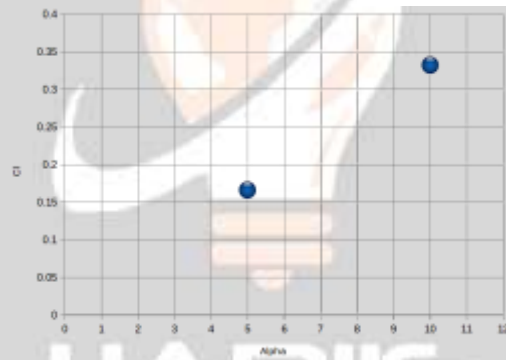


Fig. 26. OpenFOAM

Thus, by studying the above results, the solvers for OpenFOAM and OpenVSP are validated and can be used for analyzing the UAV.

F. UAV analysis:

The same technique presented above has been used for analysis of the UAV. Following figures (fig. 27, fig. 28) shows the mesh generated for both the modes.

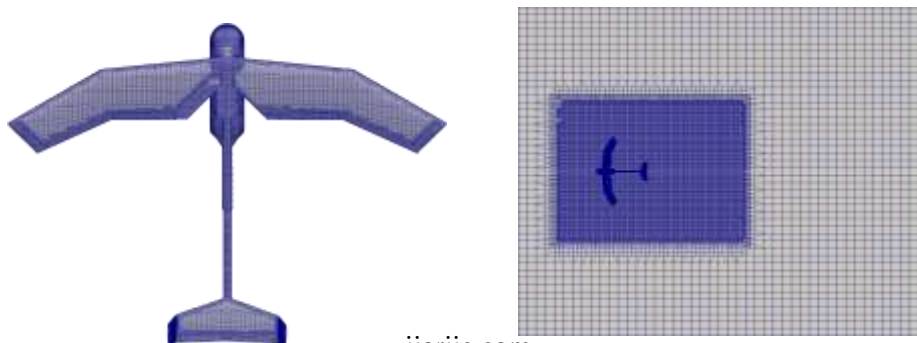


Fig. 27. Mode 1

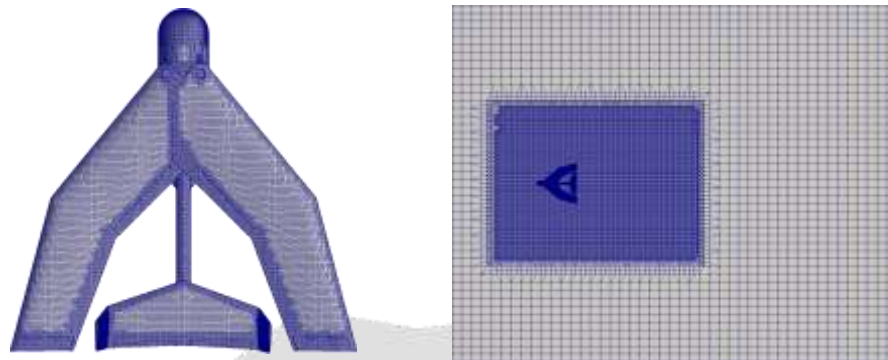


Fig. 28. Mode 2

5. Results

A. Residuals:

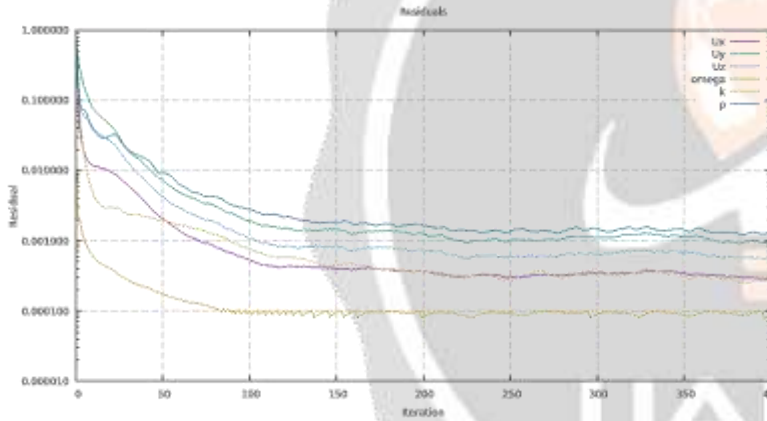


Fig. 29. Mode 1 – Residual vs Iteration

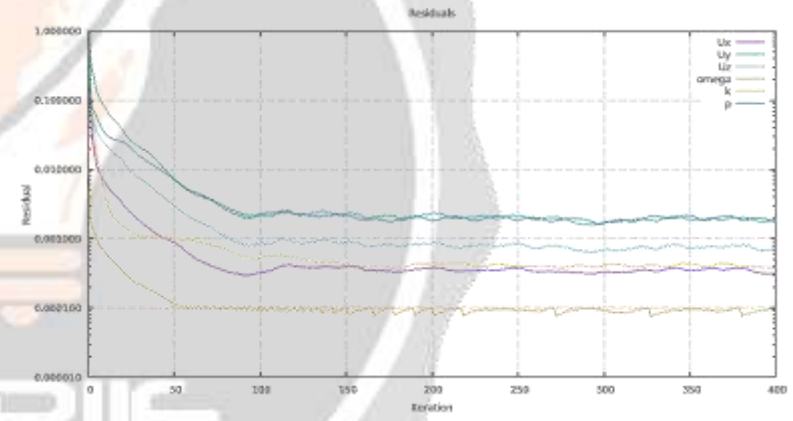


Fig. 30. Mode 2 – Residual vs Iteration

B. CI convergence:

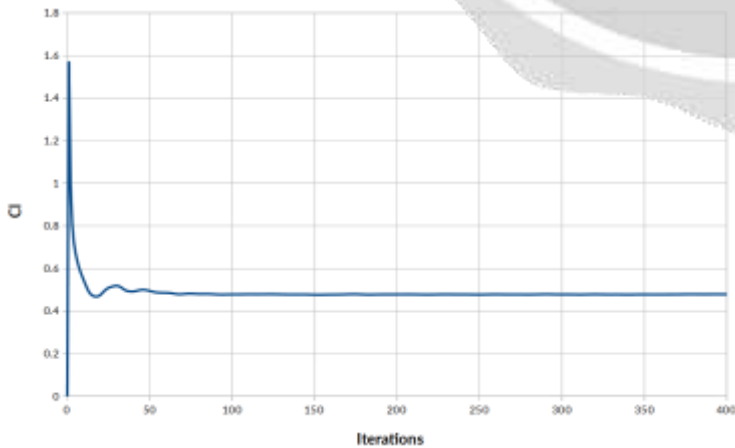


Fig. 31. Mode 1 – CI vs Iteration

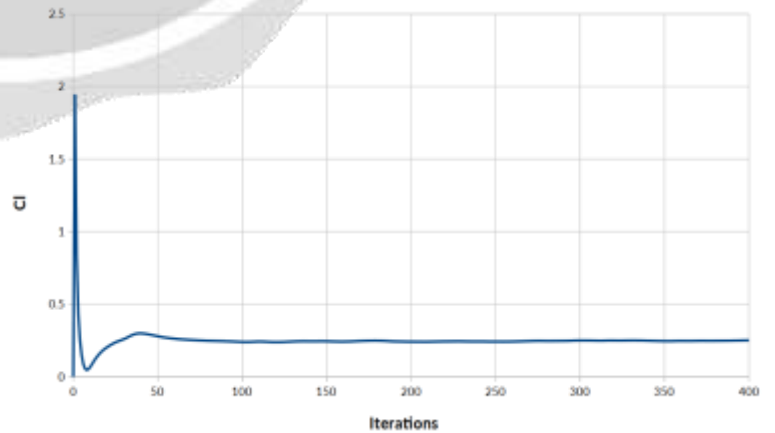


Fig. 32. Mode 2 – CI vs Iteration

C. Cd convergence:

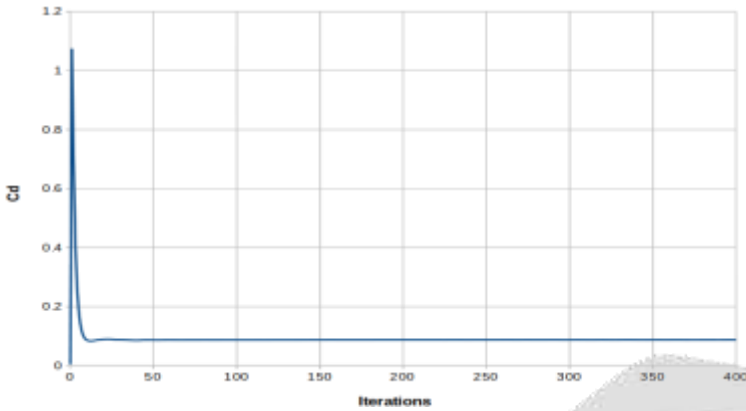


Fig. 33. Mode 1 – Cd vs Iteration

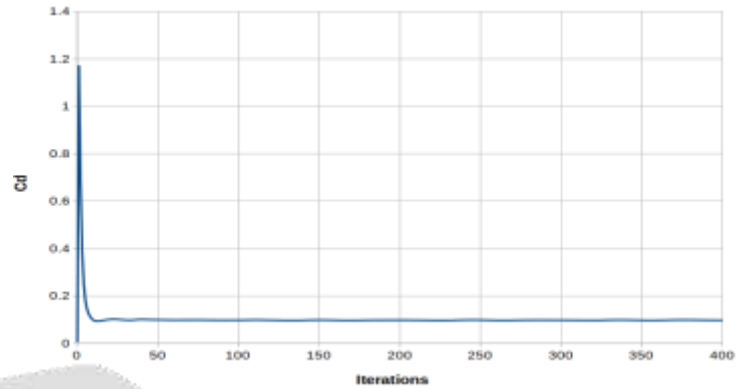
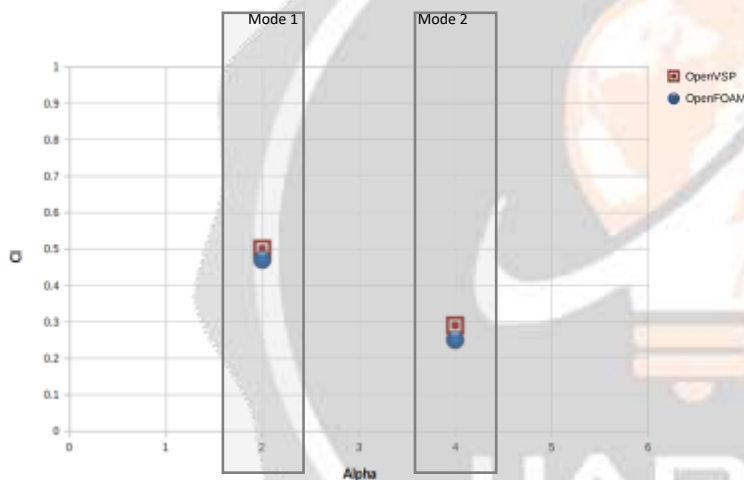


Fig. 34. Mode 2 – Cd vs Iteration

D. Comparison:

In this section, the results for both the modes are compared after doing analysis using both software. The following graph (fig. 35) shows the Cl vs Alpha comparison.

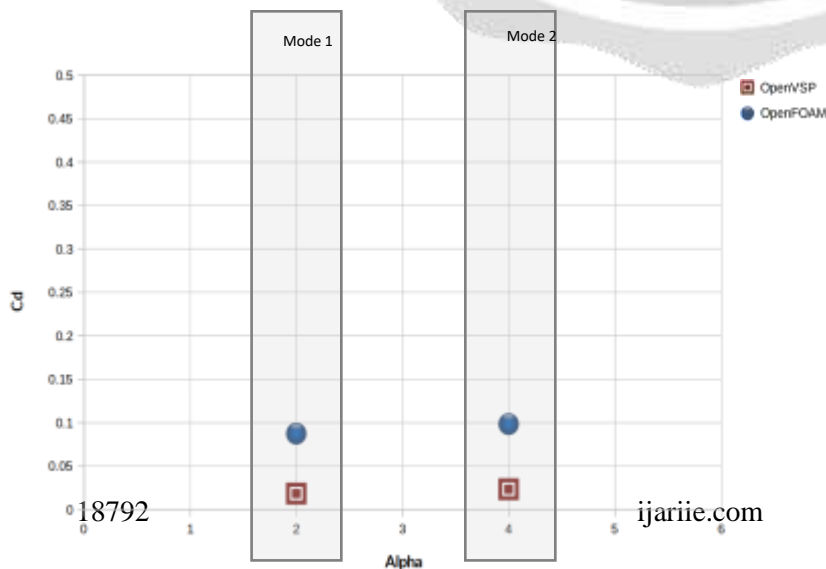


Cl Values	Neutral Angle	OpenVSP	OpenFOAM
Mode 1	2°	0.5	0.47
Mode 2	4°	0.29	0.25

Table. VII. CL Values

Fig. 35. Comparison of solvers – Cl vs Alpha

From the above table (Table VII), it is observed that, the variance in the results for CL values from both the solvers is minimum. The same can be observed for the Cd values. The following graph (fig. 36) shows the Cd Values



Cd Values	Neutral Angle	OpenVSP	OpenFOAM
Mode 1	2°	0.018	0.087
Mode 2	4°	0.023	0.098

Table. VIII. CD Values

Cd vs Alpha comparison.

Fig. 36. Comparison of solvers – Cd vs Alpha

From comparisons for both Cl and Cd values, it is observed that there is some variance in the values calculated by OpenVSP and OpenFOAM. The reason is, that OpenVSP uses VLM for calculating the force coefficients which does not consider the turbulence, or the viscosity of the flow. The Cd values have higher variance because VLM calculates only the induced drag but neglects the parasitic drag. Thus, the Cd values calculated by OpenVSP are lower as it does not have the parasitic component of the drag.

E. Flow visualization:

The UAV has a modular payload system. Meaning, the payload can be interchanged and can be fitted with specific payload for specific missions. Flow visualisation is done to analyse the flow around one of the payload designed for this project. This payload has channelling system, which is being visualised in fig. 37. The flow is colour graded using velocity values, and the UAV is colour graded using the pressure values.

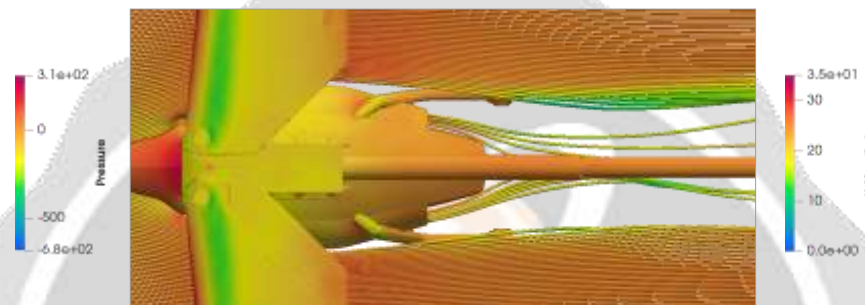


Fig. 37. Channeling

The purpose to channel the flow towards the center of the UAV is because, the propeller has its blades towards the central area. For increasing the propeller efficiency, more flow is directed towards the propellers.



Fig. 38. Flow over the tail

It is observed in fig. 38 that due to a low pressure area on top of the tail, the flow coming out of the channels is being directed towards the top of the tail. This is a good situation for the UAV as more flow is flowing over the tail helping to generate enough lifting force even at lower angles of attack. Fig. 39 shows the generation of vortices at wing tips.



Fig. 39. Vortices

6. CONCLUSIONS

The initial parameters for the UAV were calculated analytically using the historical data of the PENGUIN-C UAS by UAV Factory. These parameters were used to design an initial model of the UAV, which was the base point to start analyzing and optimizing. Before starting with the analysis process, the solvers were validated using the published data on Research Gate (Authors – Shinde, Subhash & Paul, Akshoy & Jain, Anuj).

After validation, the solvers of both software – OpenFOAM and OpenVSP were used to calculate the force coefficients using FVM and VLM techniques. These results were cross verified to find the variance. Finally, flow visualization was done to analyze the flow around the designed module.

Thus, the project – Conceptual design and analysis of a multi-functional UAV is being completed.

7. FUTURE WORK:

The contents of this project are focused on only the aerodynamic aspect of the UAV. Meaning, designing the wing, tail, modules by considering the air-flow interaction and generation of forces. But that does not make this design industry ready to be flown for actual missions. This project was conceptual design of a UAV focusing on one of the many aspects needed to bring it into reality. [14] Similarly, literature survey and research has to be done in the fields of selection of materials, manufacturing and assembling techniques, communications, and propulsion system.

8. REFERENCES

- 1) J. Porter, May 2020, "Zipline's drones are delivering medical supplies and PPE in North Carolina", <https://www.theverge.com/2020/5/27/21270351/ziplinedrones-novant-healthmedical-center-hospital-supplies-ppe>
- 2) McNeal, November 2014, "Drones and aerial surveillance: Considerations for legislatures", <https://www.brookings.edu/research/drones-and-aerialsurveillance-considerations-for-legislatures/#footnote-1>
- 3) J. H. Ong, A. Sanchez and J. Williams, "Multi-UAV System for Inventory Automation," 2007 1st Annual RFID Eurasia, 2007, pg. 1-6, doi: 10.1109/RFIDEURASIA.2007.4368142.
- 4) Shelly Singh, 2019, "Unmanned Aerial Vehicle (UAV) Market Worth \$45.8 Billion by 2025", <https://www.prnewswire.com/news-releases/unmanned-aerial-vehicle-uav-market-worth-45-8-billion-by-2025--exclusive-report-by-marketsandmarkets-300947048.html>
- 5) Abhishek A. Jadhav, "Design of a Drone Having Capability to Transform its Configuration Depending on Mission Profile", 2020, International Journal of Engineering Applied Sciences and Technology, Vol. 5, Issue 4, pg. 227-232, ISSN No. 2455-2143.
- 6) Maria de Fátima Bent, "Unmanned Aerial Vehicles: An Overview", 2019, Inside GNSS, pg. 54-61.
- 7) Hui Chen, Xiangming Zheng, Yuan Wang, "Conceptual Design Methodology for Battery-Powered Mini-UAV", 2016, Advances in Intelligent Systems Research, pg. 413-420.
- 8) H. Shakhathreh, "Unmanned Aerial Vehicles (UAVs): A Survey on Civil Applications and Key Research Challenges", 2019, IEEE Access, pg. 48572-48634.
- 9) Singhal, Gaurav & Bansod, "Unmanned Aerial Vehicle Classification, Applications and Challenges: A Review", 2018, Research Gate, Vol 7.
- 10) Andreas Schuette, Jan Vormweg & Ryan G. Maye, "Aerodynamic shaping design and vortical flow design aspects of a 53deg swept flying wing configuration", 2018, American Institute of Aeronautics and Astronautics, pg. 1-9.
- 11) P. Panagiotou & P. Kaparos, "Winglet design and optimization for a MALE UAV using CFD", 2014, Aerospace Science and Technology, Vol. 39, pg. 190-205.
- 12) Esteban Valencia & Victor Hildalg, "Innovative Propulsion Systems and CFD Simulations for Fixed Wing Aircraft", 2017, Aerial Robots - Aerodynamics, Control And Applications, pg. 65-69.
- 13) Parvathy Rajendran & Howard Smith, "Electric Propulsion System Sizing for Small Solar-powered Electric Unmanned Aerial Vehicle", 2016, International Journal of Applied Engineering Research, Vol. 11, pg. 9419-9423.
- 14) Pei-Hsiang Chung & Der-Ming Ma, "Design, Manufacturing, and Flight Testing of an Experimental Flying Wing UAV", 2019, Applied Sciences, Vol. 9, pg. 3043-3045.
- 15) Chip Wright, "Climb Segment", 2013, AOPA.
- 16) Shinde, Subhash & Paul, Akshoy & Jain, Anuj. (2013). "CFD analysis of viscous flow over delta-rectangular wing". 1-6. 10.1109/SCES.2013.6547537.